

## INVESTIGATION OF HIGH TEMPERATURE SULFURIZATION OF $\text{Cu}_2\text{ZnSnS}_4$ THIN FILMS ON Mo FOIL SUBSTRATES

J. X. XU\*, Y. Z. YANG, Y. Q. LIU

*School of Materials and Energy, Guangdong University of Technology,  
Guangzhou 510006, China*

In order to get a deeper understanding of the sulfurization process of  $\text{Cu}_2\text{ZnSnS}_4$  thin films, the high temperature ( $\geq 600$  °C) sulfurization of  $\text{Cu}_2\text{ZnSnS}_4$  thin films was investigated. The  $\text{Cu}_2\text{ZnSnS}_4$  thin films were fabricated on Mo foil substrates by sulfurization of Zn/Sn/Cu precursors. The structural, compositional, and morphological properties of thin films were studied. The results indicate that the dominant structure of thin films sulfurized at 500 and 550 °C is  $\text{Cu}_2\text{ZnSnS}_4$ . For thin films sulfurized at 600 °C, the  $\text{Cu}_2\text{ZnSnS}_4$  phase begins to decompose and the sulfur ratio in the thin film reduces. The  $\text{Cu}_2\text{ZnSnS}_4$  phase is absent when the sulfurization temperature increases to 650 °C, revealing the further decomposition reaction. The experimental results reveal the decomposition reaction of  $\text{Cu}_2\text{ZnSnS}_4$  when the sulfurization temperature is higher than 600 °C.

(Received December 30, 2015; Accepted February 9, 2016)

*Keywords:*  $\text{Cu}_2\text{ZnSnS}_4$ ; Decomposition; Sulfurization; High temperature

### 1. Introduction

Nowadays, the studies of thin film solar cells (TFSC) focus on absorber materials with low cost, less pollution, high absorption coefficient, and suitable band gap. The  $\text{Cu}(\text{In,Ga})\text{Se}_2$  thin film is the most popular absorber material and has been studied extensively [1,2]. However, the In element in  $\text{Cu}(\text{In,Ga})\text{Se}_2$  is rare in the earth abundance. By replacing the group III element by Zn and Sn and the Se element by S, the  $\text{Cu}_2\text{ZnSnS}_4$  thin film is novel solar cell material [3-5]. All the elements in  $\text{Cu}_2\text{ZnSnS}_4$  thin film are earth-abundant and environmentally friendly. The  $\text{Cu}_2\text{ZnSnS}_4$  thin films have high absorption coefficient above  $10^4$   $\text{cm}^{-1}$  in the visible region and band gap of about 1.5 eV [6-8]. The highest conversion efficiency of  $\text{Cu}_2\text{ZnSnS}_4$ -based thin film solar cells is 12.6% [9].

In order to improve the properties of  $\text{Cu}_2\text{ZnSnS}_4$  thin film solar cells, a deeper understanding of the growth mechanism of  $\text{Cu}_2\text{ZnSnS}_4$  is necessary. The two-step method of sulfurization of prepared Cu-Zn-Sn or Cu-Zn-Sn-S precursors is typically utilized for the fabrication of  $\text{Cu}_2\text{ZnSnS}_4$  thin films [8,10]. The sulfurization of  $\text{Cu}_2\text{ZnSnS}_4$  is more complex than the selenization of  $\text{Cu}(\text{In,Ga})\text{Se}_2$ . Most of reported  $\text{Cu}_2\text{ZnSnS}_4$  thin films use soda-lime glass as substrate, which limits the sulfurization temperature to lower than 600 °C [8,11-13]. It's interesting to study the properties of  $\text{Cu}_2\text{ZnSnS}_4$  sulfurized at higher than 600 °C. The sulfurization temperature can be increased to higher than 600 °C by using heat-resistant substrates, such as Mo

---

\*Corresponding author xujiaxiong@gdut.edu.cn

foil, stainless steel foil, and quartz glass, etc. In our previous work, we have used vacuum-based method to fabricate  $\text{Cu}_2\text{ZnSnS}_4$  thin films on Mo foil substrate [14]. Using Mo foil substrate, the  $\text{Cu}_2\text{ZnSnS}_4$  thin films show flexible properties. But the effect of high sulfurization temperature on the properties of thin films on Mo foil substrate has not been studied.

In present work, we deposited  $\text{Cu}_2\text{ZnSnS}_4$  thin films on Mo foil substrate by magnetron sputtering plus post-sulfurization. The sulfurization temperature was changed from 500 to 650 °C to analyze the impact of high temperature sulfurization treatment on thin film structures and compositions.

## 2. Experimental method

The substrates used in this experiment were Mo foils with a thickness of 50  $\mu\text{m}$  and size of  $1.25 \times 2 \text{ cm}^2$ . The Zn, Sn, and Cu thin films were successively sputtered on the Mo foils to fabricate Zn/Sn/Cu precursors. The Zn, Sn, and Cu targets (99.99% in purity) were used as source materials for sputtering. The base pressure and working pressure in the chamber were  $4.0 \times 10^{-4} \text{ Pa}$  and 0.5 Pa, respectively. During sputtering, the flow of pure argon was 20 mL/min. The Zn and Cu thin films were deposited by direct-current sputtering. The radio frequency sputtering was performed for the preparation of Sn thin films. Detail procedure of sputtering can be seen in Refs. [14,15].

After sputtering, the Zn/Sn/Cu precursors were sulfurized in a tube furnace. The tube is open type and its diameter and length are 3 and 90 cm, respectively. The solid sulfur powders (purity: 99.95% and mass: 1 g) and Zn/Sn/Cu precursors were placed in a capped quartz boat. The sulfur powders were adjacent to the precursors. Then, the quartz boat was putted in the center of tube furnace. During sulfurization, the pure  $\text{N}_2$  with a flow of 250 mL/min was introduced into the tube furnace as protective gas. The sulfurization treatments were performed under atmospheric pressure. The ramp-up rate of furnace temperature was 20 °C/min. The target sulfurization temperature was changed from 500 to 650 °C. At the target temperature, the time of sulfurization treatment was fixed at 20 min. After sulfurization treatment, the samples naturally cooled down in the  $\text{N}_2$  atmosphere.

The structural properties of the fabricated thin films were identified by X-ray diffractometry (XRD, Rigaku D/MAX-Ultima IV,  $\text{Cu-K}\alpha$  radiation) and Raman spectroscopy (HORIBA Jobin Yvon, LabRAM HR800,  $\lambda=633 \text{ nm}$ ). The compositions of thin films were measured by energy dispersive spectroscopy (EDS, Oxford, INCA350X-Max50). The morphologies of thin films were observed by scanning electron microscopy (SEM, Hitachi S3400N).

## 3. Results and discussion

Fig. 1 shows the XRD patterns of thin films sulfurized at various temperatures. The strong peaks located at  $58.6^\circ$  and  $73.7^\circ$  are original from the Mo foil substrates. For the thin films sulfurized at 500 and 550 °C, their XRD patterns can match with the standard XRD pattern of kesterite  $\text{Cu}_2\text{ZnSnS}_4$  (PDF#26-0575). The peaks located at  $18.2^\circ$ ,  $28.5^\circ$ ,  $33.0^\circ$ ,  $47.3^\circ$ , and  $56.2^\circ$  come from the (101), (112), (200), (220), and (312) planes of  $\text{Cu}_2\text{ZnSnS}_4$ , respectively. The preferred orientation of  $\text{Cu}_2\text{ZnSnS}_4$  is the (112) plane, which is in agreement with the reported results on Mo foil and other substrates [14-17]. The thin films sulfurized at 550 °C show stronger  $\text{Cu}_2\text{ZnSnS}_4$  peak. The full width at half maximum (FWHM) of the (112) peak is  $0.231^\circ$  and  $0.213^\circ$  when the sulfurization temperatures are 500 and 550 °C, respectively. According to the Debye-Scherrer equation, the calculated grain sizes are 35.1 and 38.0 nm for thin films sulfurized at 500 and 550 °C, respectively. The results indicate that the prepared thin films exhibit improved crystallinity for sulfurization temperature of 550 °C. However, these  $\text{Cu}_2\text{ZnSnS}_4$  peaks also match with the secondary phases of  $\text{Cu}_2\text{SnS}_3$  and ZnS due to the similar crystalline structures among

$\text{Cu}_2\text{ZnSnS}_4$ ,  $\text{Cu}_2\text{SnS}_3$ , and  $\text{ZnS}$ . Therefore, Raman scattering measurement was performed as an auxiliary way to characterize the phase structure of thin films. The Raman spectra of thin films are shown in Fig. 2. As seen in Fig. 2, when the sulfurization temperatures are 500 and 550 °C, the Raman peaks of  $\text{Cu}_2\text{ZnSnS}_4$  can be detected at the Raman shifts of 264, 288, 338, and 367  $\text{cm}^{-1}$ . The strongest  $\text{Cu}_2\text{ZnSnS}_4$  peak at 338  $\text{cm}^{-1}$  is consistent with our previous works and other group's works [14,15,18,19]. The Raman peaks of  $\text{Cu}_2\text{ZnSnS}_4$  are also higher for thin films sulfurized at 550 °C, revealing a better degree of sulfurization at 550 °C. In addition to the  $\text{Cu}_2\text{ZnSnS}_4$  characteristic peaks, the peaks at 142, 167, 303, and 323  $\text{cm}^{-1}$  are attributed to the secondary phases of  $\text{Cu}_x\text{S}$ ,  $\text{SnS}$ ,  $\text{Cu}_2\text{SnS}_3$ , and  $\text{Cu}_3\text{SnS}_4$ , respectively. However, the peak intensities of secondary phases are much lower than that of  $\text{Cu}_2\text{ZnSnS}_4$  peaks. Therefore, the  $\text{Cu}_2\text{ZnSnS}_4$  phase is dominant in the fabricated thin films.

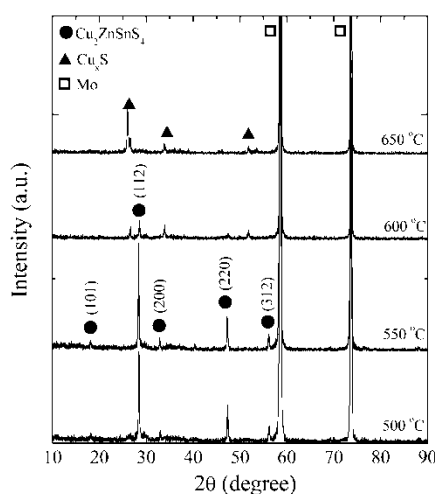


Fig. 1 The XRD patterns of thin films sulfurized at 500 to 650 °C.

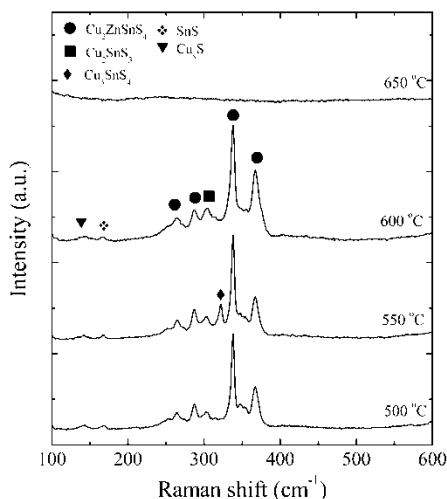


Fig. 2 The Raman scattering spectra of thin films sulfurized at 500 to 650 °C.

When the sulfurization temperature increases to 600 °C, in Fig. 1, the peaks at 28.5° and 47.3° reduce as compared with those sulfurized at 500 and 550 °C. The  $\text{Cu}_2\text{ZnSnS}_4$  peaks located at 18.2°, 33.0°, and 56.2° are absent in the XRD pattern. Besides, three new peaks can be detected at 26.6°, 34.0°, and 51.9°. The peak at 26.6° can be identified to  $\text{Sn}_3\text{S}_4$ ,  $\text{Cu}_4\text{SnS}_4$ ,  $\text{Cu}_2\text{S}$ ,  $\text{CuZn}$ ,  $\text{Cu}_7\text{S}_4$ , or  $\text{Sn}_2\text{S}_3$  phases. Its origin cannot be confirmed solely by the XRD measurement. The peak

at  $34.0^\circ$  may come from the  $\text{Cu}_{1.92}\text{S}$ ,  $\text{Cu}_7\text{S}_4$ , or  $\text{Cu}_{0.61}\text{Zn}_{0.39}$  structures and the peak at  $51.9^\circ$  may attribute to the  $\text{Cu}_{1.92}\text{S}$ ,  $\text{Cu}_9\text{S}_5$ ,  $\text{Cu}_7\text{S}_4$ , or  $\text{Sn}_3\text{S}_4$  phases. The reduced  $\text{Cu}_2\text{ZnSnS}_4$  peaks and the present peaks of secondary phases indicate that the  $\text{Cu}_2\text{ZnSnS}_4$  structure begins to decompose at the sulfurization temperature of  $600^\circ\text{C}$ . In the Raman spectrum, the detected Raman peaks of  $\text{Cu}_x\text{S}$ ,  $\text{SnS}$ ,  $\text{Cu}_2\text{SnS}_3$ , and  $\text{Cu}_2\text{ZnSnS}_4$  are similar with those of thin films sulfurized at lower temperatures. Therefore, the XRD peaks at  $26.6^\circ$ ,  $34.0^\circ$ , and  $51.9^\circ$  are all original from the secondary phase of  $\text{Cu}_x\text{S}$ . For the thin films sulfurized at  $650^\circ\text{C}$ , all the  $\text{Cu}_2\text{ZnSnS}_4$  peaks are absent in the XRD pattern. Besides, the peak at around  $26.6^\circ$  enhances significantly as compared with that of thin films sulfurized at  $600^\circ\text{C}$ . The disappearance of  $\text{Cu}_2\text{ZnSnS}_4$  peak and the enhanced secondary phases indicate that the decomposition of  $\text{Cu}_2\text{ZnSnS}_4$  enhances for sulfurization temperature increased to  $650^\circ\text{C}$ . The  $\text{Cu}_2\text{ZnSnS}_4$  peaks also disappear in the Raman spectrum. Only a rather weak peak of  $\text{Sn}_2\text{S}_3$  is detected at the Raman shift of  $241\text{ cm}^{-1}$ . The decomposer  $\text{SnS}$  is sulfurized to form  $\text{Sn}_2\text{S}_3$ .

According to the results of XRD and Raman measurements, the phase structures and sulfurization statuses of the prepared thin films are summarized in Table 1. The formation and decomposition of  $\text{Cu}_2\text{ZnSnS}_4$  happen successively when the sulfurization temperature increases from  $500$  to  $650^\circ\text{C}$ .

Table 1 The structures and sulfurization statuses of thin films with the change of sulfurization temperature.

Sulfurization temperature ( $^\circ\text{C}$ )	Thin film structure	Sulfurization status
500	$\text{Cu}_2\text{ZnSnS}_4$ , $\text{Cu}_2\text{SnS}_3$ , $\text{Cu}_x\text{S}$ , $\text{SnS}$	Formation
550	$\text{Cu}_2\text{ZnSnS}_4$ , $\text{Cu}_2\text{SnS}_3$ , $\text{Cu}_3\text{SnS}_4$ , $\text{Cu}_x\text{S}$ , $\text{SnS}$	Enhanced formation
600	$\text{Cu}_2\text{ZnSnS}_4$ , $\text{Cu}_2\text{SnS}_3$ , $\text{Cu}_x\text{S}$ , $\text{SnS}$	Decomposition
650	$\text{Cu}_x\text{S}$ , $\text{Sn}_2\text{S}_3$	Enhanced decomposition

For the compositional properties of thin films, the measured EDS results of the prepared thin films sulfurized at different temperatures are shown in Fig. 3. Fig. 3(a) presents the atomic ratios of Cu, Zn, Sn, and S elements of thin films. The values of  $\text{Cu}/(\text{Zn}+\text{Sn})$ ,  $\text{Zn}/\text{Sn}$ , and  $\text{S}/\text{metal}$  are shown in Fig. 3(b). During the EDS measurement, we only concerned the Cu, Zn, Sn, and S elements for the calculation of thin film composition. For the thin films sulfurized at  $500$  and  $550^\circ\text{C}$ , their measured compositions are near the stoichiometry of  $\text{Cu}_2\text{ZnSnS}_4$ , indicating the formation of  $\text{Cu}_2\text{ZnSnS}_4$ . When the sulfurization temperature increases to  $600$  and  $650^\circ\text{C}$ , a significant reduction in the sulfur ratio is detected. The sulfur ratio is only  $30.21\%$  when the sulfurization temperature is  $650^\circ\text{C}$ . The reduced sulfur ratio suggests the decomposition of  $\text{Cu}_2\text{ZnSnS}_4$ .

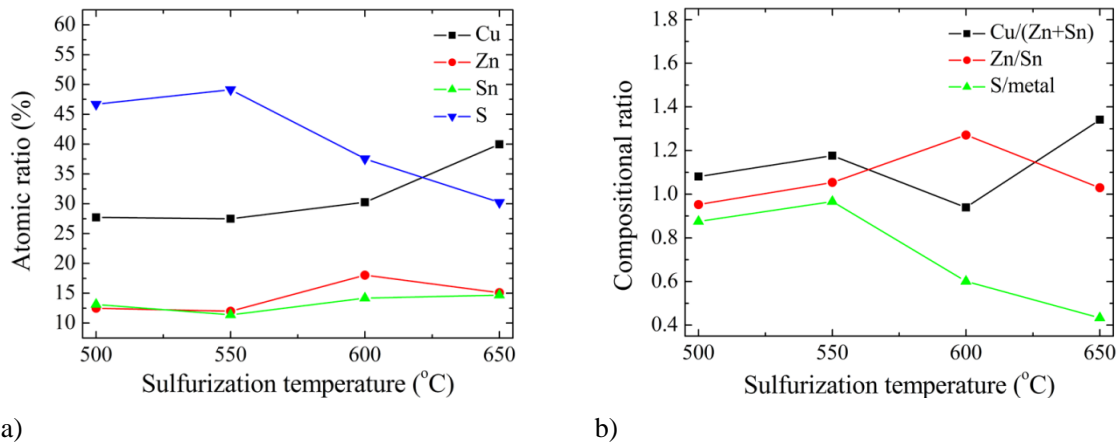


Fig. 3 (a) The atomic ratios of Cu, Zn, Sn, and S elements and (b) the values of  $\text{Cu}/(\text{Zn}+\text{Sn})$ ,  $\text{Zn}/\text{Sn}$ , and  $\text{S}/\text{metal}$  of thin films with sulfurization temperature

Fig. 4 shows the surface SEM images of the prepared thin films. For the  $\text{Cu}_2\text{ZnSnS}_4$  thin films sulfurized at 500 °C, the thin film surface is homogeneous while some voids are presented. But cracks are not observed in the SEM images. The grainy morphologies can be obviously detected and the grain size is about 500 nm. In addition, some grains coalesce. When the sulfurization temperature increases to 550 °C, the surfaces of thin films become more compact. Besides, the grain size increases when the sulfurization temperature varies from 500 to 550 °C. For the thin films sulfurized at 600 and 650 °C, the voids in the surface increase. It is ascribed to the decomposition of  $\text{Cu}_2\text{ZnSnS}_4$  structure. The voids may result from the volatilization of SnS and sulfur.

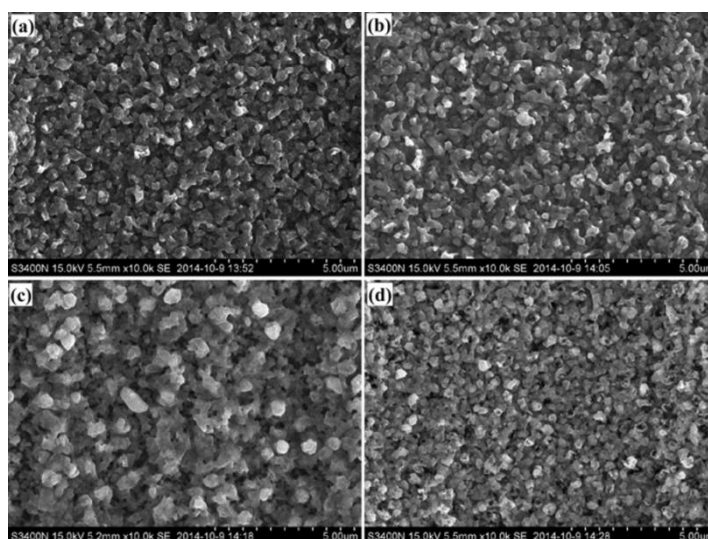


Fig. 4 The SEM images of thin films sulfurized at (a) 500, (b) 550, (c) 600, and (d) 650 °C.

#### 4. Conclusion

The Zn/Sn/Cu precursors were sputtered on Mo foil substrates and then sulfurized. The sulfurization temperatures changed from 500 to 650 °C. The properties of the prepared thin films were measured by XRD, Raman, EDS, and SEM to investigate the effect of high temperature sulfurization. The results show that the phase structures of thin films sulfurized at 500 and 550 °C are  $\text{Cu}_2\text{ZnSnS}_4$  as well as traces of secondary phases. The crystallinity of thin films sulfurized at 550 °C is higher than that of thin films sulfurized at 500 °C. These thin films are near-stoichiometric and composed of grains in the surface. For thin films sulfurized at 600 and 650 °C, the  $\text{Cu}_2\text{ZnSnS}_4$  phase decomposes with the increasing sulfurization temperature, resulting in decreasing sulfur atomic ratio. The  $\text{Cu}_2\text{ZnSnS}_4$  phase is absent when the sulfurization temperature is 650 °C. The study of high temperature sulfurization of  $\text{Cu}_2\text{ZnSnS}_4$  can contribute to deeper understanding of the sulfurization mechanism of  $\text{Cu}_2\text{ZnSnS}_4$ .

## Acknowledgements

This work was funded by National Natural Science Foundation of China (No. 61504029) and Doctoral Starting up Foundation of Guangdong University of Technology (No. 15ZK0011).

## References

- [1] M. Powalla, W. Witte, P. Jackson, S. Paetel, E. Lotter, R. Wuerz, F. Kessler, C. Tschamber, W. Hempel, D. Hariskos, *IEEE J. Photovolt.* **4**, 440 (2014).
- [2] P. Jackson, D. Hariskos, R. Wuerz, W. Wischmann, M. Powalla, *Phys. Status Solidi RRL* **8**, 219 (2014).
- [3] Y. X. Zhao, C. Burda, *Energy Environ. Sci.* **5**, 5564 (2012).
- [4] T. Todorov, O. Gunawan, S. J. Chey, T. G. de Monsabert, A. Prabhakar, D. B. Mitzi, *Thin Solid Films* **519**, 7378 (2011).
- [5] T. Wada, S. Nakamura, T. Maeda, *Prog. Photovolt: Res. Appl.* **20**, 520 (2012).
- [6] M. Cao, L. Li, B. L. Zhang, J. Huang, L. J. Wang, Y. Shen, Y. Sun, J. C. Jiang, G. J. Hu, *Sol. Energy Mater. Sol. Cells* **117**, 81 (2013).
- [7] K. V. Gurav, J. H. Yun, S. M. Pawar, S. W. Shin, M. P. Suryawanshi, Y. K. Kim, G. L. Agawane, P. S. Patil, J. H. Kim, *Mater. Lett.* **108**, 316 (2013).
- [8] C. Gao, H. L. Shen, F. Jiang, H. Guan, *Appl. Surf. Sci.* **261**, 189 (2012).
- [9] W. Wang, M. T. Winkler, O. Gunawan, T. Gokmen, T. K. Todorov, Y. Zhu, D. B. Mitzi, *Adv. Energy Mater.* **4**, 1301465 (2014).
- [10] N. Momose, M. T. Htay, T. Yudasaka, S. Igarashi, T. Seki, S. Iwano, Y. Hashimoto, K. Ito, *Jpn. J. Appl. Phys.* **50**, 01BG09 (2011).
- [11] X. Jiang, L. X. Shao, J. Zhang, D. Li, W. Xie, C. W. Zou, J. M. Chen, *Surf. Coat. Technol.* **228**, S408 (2013).
- [12] K. Tanaka, T. Shinji, H. Uchiki, *Sol. Energy Mater. Sol. Cells* **126**, 143 (2014).
- [13] F. Y. Liu, K. Zhang, Y. Q. Lai, J. Li, Z. A. Zhang, Y. X. Liu, *Electrochem. Solid-State Lett.* **13**, H379 (2010).
- [14] J. X. Xu, Z. M. Cao, Y. Z. Yang, Z. W. Xie, *J. Mater. Sci.: Mater. Electron.* **26**, 726 (2015).
- [15] J. X. Xu, Z. M. Cao, Y. Z. Yang, Z. W. Xie, *J. Renew. Sustain. Energy* **6**, 053110 (2014).
- [16] A. Khalkar, K. S. Lim, S. M. Yu, S. P. Patole, J. B. Yoo, *Electron. Mater. Lett.* **10**, 43 (2014).
- [17] J. H. Tao, J. He, K. Z. Zhang, J. F. Liu, Y. C. Dong, L. Sun, P. X. Yang, J. H. Chu, *Mater. Lett.* **135**, 8 (2014).
- [18] A. Wangperawong, J. S. King, S. M. Herron, B. P. Tran, K. Pangan-Okimoto, S. F. Bent, *Thin Solid Films* **519**, 2488 (2011).
- [19] U. Chalapathi, S. Uthanna, V. Sundara Raja, *J. Renew. Sustain. Energy* **5**, 031610 (2013).